An Evanescent Hybrid Silicon Laser Neuron

Mitchell A. Nahmias, Alexander N. Tait, Bhavin J. Shastri, and Paul R. Prucnal
Lightwave Communications Laboratory, Department of Electrical Engineering, Princeton University, Princeton, NJ 08544, USA
mnahmias@princeton.edu

***Abstract*—We propose a hybrid silicon laser and photodetector system that can emulate the electro-physiological behavior of a real neuron at ultrafast time-scales. Networks of lasers would scale up easily using a silicon III-V wafer-bonding platform.**

I. Introduction

Neuromorphic networks have experienced a surge of popularity over the last twenty years, motivated in part by bringing computation closer to its underlying physics [1]. Scaling to larger numbers of neurons, however, requires prohibitively complex networks in which there is a fundamental density-bandwidth trade-off. Alternatively, photonic systems can potentially offer much higher bandwidths and lower energy usage than electronics, making the spike-based approach to information processing a perfect fit for the technology. Today, there are a growing number of applications that require higher speeds and lower latencies that may be outside the abilities of the fastest electronic circuits, including processing of the RF spectrum or ultrafast control. Taking advantage of the ephemeral dynamics in photonic systems such as those in lasers could lead to processors that operate on picosecond time scales. In addition, there is a close analogy between the dynamics of lasers and those of biological systems, both of which can exhibit excitability [2].

Here, we propose a hybrid silicon distributed feedback (DFB) laser and photodetector system that can emulate both a Leaky Integrate-and-Fire (L&F) neuron and a synaptic variable, completing a computational paradigm that can be used to emulate a wide variety of functional cortical algorithms [3]. Lasers offer a speed increase of about seven orders of magnitude, outpacing both biological and electronic systems. Networks of such devices are easily scalable using a silicon III-V wafer-bonding platform [4].

II. Device Description

As illustrated in Fig. 1, the device consists of three primary components: two photodetectors and an excitable laser. The photodetectors receive optical pulses from a network and produce a push-pull current signal which modulates the laser carrier injection. The excitable laser acts as a threshold decision maker and clean pulse generator analogous to the neural axon hillock. A simple model of a single-mode laser with saturable absorber (SA) section has been proven to be analogous to the equations governing an L&F neuron in certain parameter regimes [2]. We chose to implement this model using a hybrid silicon evanescent DFB laser [5], the device on the left in Fig. 2. The photodetector front-end proposed in this paper adds full synaptic conduction dynamics that greatly improve the capabilities and biological accuracy of the laser neuron.

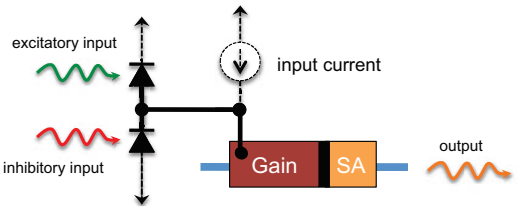

Fig. 1. A circuit diagram of the proposed device. Excitatory and inhibitory inputs are incident on photodetectors, which represent synaptic variables. The induced photocurrent modulates carrier injection into a laser with embedded saturable absorber, which may cause the laser to transmit a pulse back into the network. The resulting output travels to other devices in the network. Dotted lines represent low-frequency pumping and bias wires.

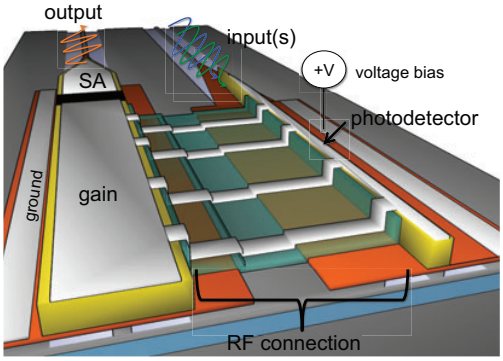

Fig. 2. Cross-section of a silicon hybrid evanescent laser neuron design. Optically active III-V components are bonded to an SOI substrate with rib waveguides. Optical spikes of potentially multiple wavelengths are incident onto the photodetector (right) from a passive SOI network. The resulting RF current pulse modulates the gain section of a two-section laser (left). (Inhibitory photodetector and pumping current source not shown for simplicity.) Legend : Si (gray), dielectric insulator (blue), III-V lower etch level (orange), III-V upper etch level (yellow), metal (white), proton implanted III-V (black).

Much of the energy cost of electronic conversion in optical systems comes from the need for high-speed clocked transistor circuitry and the need to demultiplex WDM channels before conversion. In our case, electronic conversion does not have the goal of signal regeneration, but instead of exploiting electronic physics for intermediate analog processing. The use of passive integrated electrical wires does not sacrifice bandwidth or sensitivity in this device. Pulse reshaping is not required due to the clean pulse generation in the excitable laser. The conversion between optical and electronic domains also cutails the propagation of optical phase noise and the need for direct wavelength conversion, thus eliminating two major

978-1-4577-1507-5/13/$26.00 ©2013 IEEE

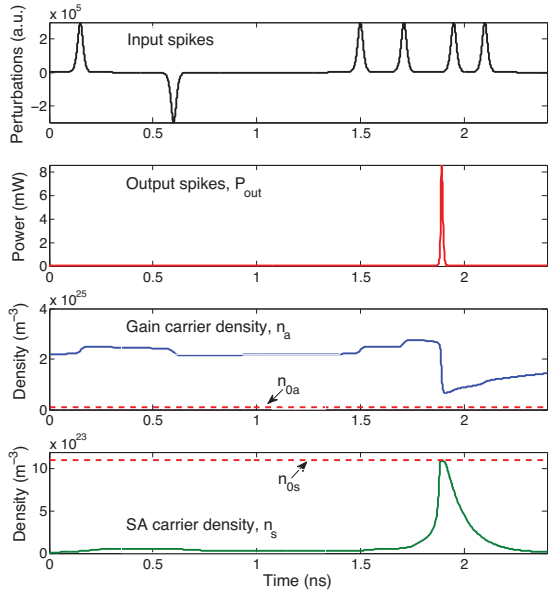

Fig. 3. A simulation of a DFB laser neuron with realistic parameters. Current perturbations from the photodetector (input spikes) modulate the gain (in blue). Enough excitatory activity causes the release of a pulse, followed by a short refractory period. This behavior mirrors that of an L&F neuron.

barriers facing scalable optical computing [6]. Every device in the primary signal pathway performs both physical and computational roles, resulting in a robust, ultrafast, expressive, and extremely efficient signal processing primitive.

1) The Neural Front-End: Inputs from other laser neurons are weighted in the optical domain before reaching the excitatory or inhibitory photodetector. Each photodetector produces a photocurrent summing the total optical power. Demultiplexing many input channels is not necessary because the incoherent sum of all WDM channels within the InP detection band is intentionally computed by the photodetector. Photodetectors have been demonstrated on the same hybrid silicon evanescent platform used for laser gain sections with response times limited by parasitic capacitance [7].

Dynamics introduced by the photodetector are analogous to synaptic dynamics governing the concentration of neurotransmitters in between signaling biological neurons. Photocurrent flow in a real photodiode and neural synaptic dynamics can be modeled by a first-order low-pass filter [8]. Photodetector time constants can be controlled with different biasing and device dimensions, and can be varied to obtain a large repertoire of processing behaviors. Recently, evanescent photodetector bandwidths up to 30GHz have been demonstrated [9].

Analog excitatory and inhibitory photocurrents are subtracted passively by a push-pull wire junction. The net photocurrent conducts over a short wire to modulate the laser gain section. These wires are roughly analogous to passive dendritic conduction, with the key difference that there are only two wires regardless of the number of input channels. The sensitivity-bandwidth of the neural front-end is not significantly reduced during electronic conversion and passive processing, although transmission lines can suffer from many effects that render them unsuitable for high-bandwidth interconnects. Distortions introduced by impedance mismatch, attenuation, dispersion, and radiative interference coupling are all negligible for wires much shorter than the signals of interest. We employ a co-integrated wire design to keep the electronic connection local. A 20μm wire has a characteristic conduction delay of nearly 10THz, and will not introduce significant transmission line distortion for sub-THz signals.

2) The Excitable Laser: A two-section DFB hybrid evanescent laser is used to implement excitable dynamics. The DFB cavity has a single longitudinal lasing mode and allows lithographic definition of lasing wavelength via SOI grating pitch. A proton implantation region electrically isolates the semiconductor absorber and gain sections. Small modulation currents that exceed the Q-switch threshold will trigger large pulse discharges. We use a standard two-section laser rate equation to model the described device:

$$\frac{dN_{ph}}{dt} = \Gamma_a g_a(n_a - n_{0a})N_{ph} + \Gamma_s g_s(n_s - n_{0s})N_{ph} - \frac{N_{ph}}{\tau_{\rm ph}} + V_a \beta B_r n_a^2 \quad (1a)$$

$$\frac{dn_a}{dt} = -\Gamma_a g_a(n_a - n_{0a})\frac{N_{ph}}{V_a} - \frac{n_a}{\tau_a} + \frac{I_a + i_e(t)}{eV_a} \quad (1b)$$

$$\frac{dn_s}{dt} = -\Gamma_s g_s(n_s - n_{0s})\frac{N_{ph}}{V_s} - \frac{n_s}{\tau_s} + \frac{I_s}{eV_s} \quad (1c)$$

where $N_{ph}(t)$ is the total number of photons in the cavity, $n(t)$ is the number of carriers, n_0 is the transparency carrier density, V is the cavity volume, Γ is the confinement factor, τ is the carrier lifetime, τ_p is the photon lifetime, g is the differential gain/loss, β is the spontaneous emission coupling factor, B_r is the Bimolecular recombination term, and $i_e(t)$ represents the electrical modulation in the gain provided by the photodetector system. Subscripts a and s identify the active and absorber regions. We use realistic parameters, based on those found in [2], [5], [7]. The results are shown in Fig. 3.

III. Conclusion

The results included therein have demonstrated that it is possible to design a hybrid silicon laser that emulates biological networks of neurons at ultrafast speeds and on a scalable platform. The L&F model with a synaptic variable, coupled with tunable routing in a passive SOI network on a scalable platform, could potentially emulate a huge variety of cortical functions, including control systems, semantic pointers, and high dimensional feature extraction of input data [10].

References

[1] G. Indiveri et al., Front Neurosci., **5**, 1 (2011).
[2] M. A. Nahmias et al., IEEE J. Sel. Topics Quantum Electron. **19** (2013).
[3] C. Eliasmith, Neural Comput., **17**, 1276 (2005).
[4] J. E. Bowers et. al., Optics and Photonics News, **21**, 28 (2010).
[5] A. Wang et al., Opt. Exp., **16**, 4413 (2008).
[6] D. G. Feitelson, *Optical Computing*, Cambridge, MA: MIT Press (1988).
[7] H. Park et al., Opt. Exp., **15**, 6044 (2007).
[8] A. Destexhe et al., "Kinetic models of synaptic transmission," in *Methods in Neuronal Modelling*, Cambridge, MA: MIT Press (1998).
[9] A. Beling et al., Proc. OFC'13, OM2J (2013).
[10] C. Eliasmith et al., Science, **338**, 1202 (2012).